DOI: 10.1002/ejic.200900669

Stable Selenenium Cations: Unusual Reactivity and Excellent Glutathione Peroxidase-Like Activity

Vijay P. Singh,[a] Harkesh B. Singh,*[a] and Ray J. Butcher[b]

Keywords: Selenenium / Selenium / Glutathione peroxidase / Ebselen / Enzyme models / Density functional calculations

The syntheses of the three selenenium cations **17**–**19** derived from *N*-[*n*-butyl-(3-nitrobenzylimino)]phenyl selenide (**14**) are described. Precursor **14** was synthesized by treating *N*-(2-bromo-3-nitrobenzylimino)benzene (**12**) with in situ generated *n*BuSeNa. The selenenium cation **17** with chloride as counteranion was isolated when **14** was treated with sulfuryl chloride (SO_2Cl_2) in the presence of triethylamine (Et_3N). The selenenium cations with bromide (**18**) and tribromide (**19**) as counteranions, were synthesized by treating **14** with Br_2 in the presence of Et_3N. Reaction of **19** with thiophenol afforded two unexpected products: the cyclic diselenide **20** and the bicyclic selenide **21**. Oxidation of **18** with hydrogen peroxide afforded the ebselen derivative, 2-(4-bromophenyl)-7-nitro-1,2-benzisoselenazol(2*H*)-3-one *Se*-oxide (**22**). The presence of nonbonding Se···O/Se–N intramolecular interactions in **18** and **19** have been confirmed by single-crystal X-ray studies. Glutathione peroxidase-like antioxidant activities of **17**–**19** and related compounds have been determined by the coupled reductase assay. It is proved that the high GPx-like activities of cations involve the formation of corresponding intermediate selenoxide in the catalytic cycle. The isolated selenoxide **22** shows the highest GPx-like activity among the series of compounds. The compounds have been further investigated by density functional theory calculations at the B3LYP level of theory using the 6-31+G(d) basis set to identify nonbonding Se···O/N interactions. The second perturbation energy was obtained through natural bond orbital (NBO) analysis and NBO charges were calculated to ascertain the positive charge at the selenium atom. Nucleus-independent chemical shifts (NICS) calculations have also been carried out.

Introduction

Organoselenium compounds stabilized by intramolecular nonbonding interactions have attracted considerable interest as chiral reagents in asymmetric organic synthesis,[1,2] and selenoenzyme glutathione peroxidase (GPx) mimetics.[3] Ebselen [PZ 51, 2-phenyl-1,2-benzisoselenazol-3-(2*H*)-one], a Se–N heterocyclic compound is a clinically useful antioxidant and antiinflammatory agent.[3f,3i,4] Recently, much attention has been directed towards the synthesis of several other organoselenium compounds that mimic the activity of GPx.[5–11] Electrophilic selenium reagents ($ArSe^+X^-$, where X = F, Cl, Br, BF_4, OTf, SbF_6, PF_6, OSO_3H)[2,12] are often utilized for the functionalization of olefins. For example, addition of selenium electrophiles **2** to alkenes leads to the formation of intermediate seleniranium ions **3** (Scheme 1).[2,12b] These intermediates are then attacked by nucleophiles from the *anti* side leading to selenides **4**. For better reactivity and improved selectivity toward olefins/acetylenes, several in situ generated selenenium ions ($ArSe^+X^-$) having both intramolecular coordinating groups and noncoordinating anions (BF_4^-, OTf^-, PF_6^-, OSO_3H^-, SbF_6^-, $SbCl_6^-$) have been employed.[12b,12c,12j,12n,13]

Although participation of selenenium cations ($ArSe^+$) has been postulated in all addition reactions of olefins/acetylenes, its isolation and characterization is limited to one notable study by Furukawa and coworkers.[14a] The group was the first to demonstrate the isolation and structural characterization of organoselenenium ion **5** (Figure 1) which was synthesized by the reaction of 2,6-bis[(dimethylamino)methyl]phenyl methyl selenide with *t*BuOCl/KPF_6. Ion **5** has also been prepared by Poleschner and Seppelt by reacting the precursor selenide with XeF_2/KPF_6.[12g] More recently, the group has succeeded in isolating and structurally characterizing the elusive addition intermediate, selenirenium ions **6** and its tellurium analogue with bulky, noncoordinating counteranions.[13] Both are stable enough for isolation under argon, however, decompose within a week to a significant extent. Very recently, transfer of in situ generated seleniranium group **7** from one olefin to another, has been observed by Denmark et al. using NMR spectroscopy.[14b] Back and coworkers have reported the synthesis of a Se^{IV} cation with chloride as counteranion where selenium is covalently bonded to two aryl carbons, one nitrogen atom and intramolecularly coordinated to an amide oxygen.[15]

[a] Department of Chemistry, Indian Institute of Technology, Bombay, Mumbai 400076, India
Fax: +91-22-2572-3480
E-mail: chhbsia@chem.iitb.ac.in
[b] Department of Chemistry, Howard University, Washington, DC 20059, USA

Supporting information for this article is available on the WWW under http://dx.doi.org/10.1002/ejic.200900669.

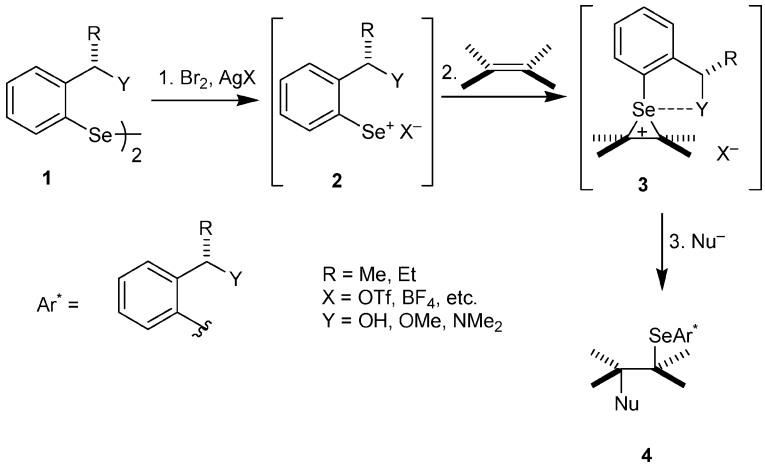

Scheme 1. Preparation of seleniranium cations **3**.

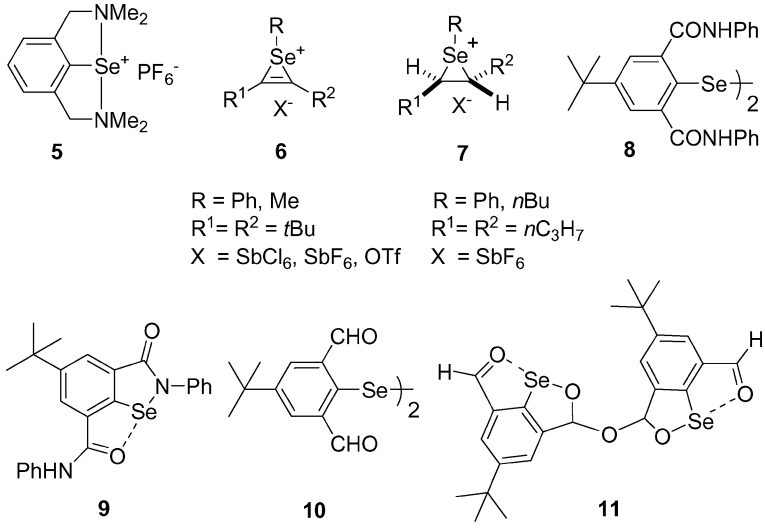

Figure 1. Selenium cations and some other organoselenium compounds stabilized by intramolecularly coordinating groups.

Our group has a long standing interest in the synthesis and reactivity of organochalcogens stabilized by a single intramolecularly coordinating group.[16] More recently, we have initiated a program to study the structure and reactivity of organoselenenyl derivatives having two *ortho*-coordinating groups.[16c–16e] Attempted isolation of diselenide **8** having two *ortho*-amide groups, afforded much sought after ebselen derivative 5-*tert*-butyl-2-phenyl-7-(phenylcarbamoyl)benzisoselenazol-3(2*H*)-one (**9**) stabilized by coordination of an amide group.[16d] Similarly, an attempted halogenation reaction of diselenide **10** led to the isolation of novel selenium (II) ester **11** stabilized by the *ortho*-formyl group.[16e] Extending the concept, we planned to isolate similar diselenides having two different coordinating groups *ortho* to the selenium such as substrate *N*-(2-bromo-3-nitrobenzylimino)benzene (**12**), with nitro and imine (–CH=N–) groups and compare its reactivity with diselenides **8** and **10** having symmetrical coordinating groups. Herein, we report the attempted synthesis of the diselenide **13** and its selenenyl halide derivatives.

Results and Discussion

Attempted synthesis of diselenide **13** by reacting **12** with in situ generated Na_2Se_2 led to a dark-green intractable mixture (Scheme 2). Therefore, unsymmetrical *N*-[*n*-butyl-(3-nitrobenzylimino)] phenyl selenide **14** was used as a precursor to generate the organoselenenyl halides and related derivatives (Scheme 2). Chlorination of **14** yielded ionic selenenium ion **17** instead of the selenenyl chloride **15**. Similarly, bromination of **14** afforded novel ionic selenenyl bromide **18** instead of the expected selenenyl bromide **16**. Formation of **17** and **18** was accompanied by *N*-phenyl ring halogenations as well. An attempt to prepare the corresponding iodide salt by the iodination of **14** with molecular iodine in chloroform was unsuccessful. When the bromination reaction of **14** was carried out with an excess of bromine and the stirring was continued for a shorter duration, the reaction afforded selenenium ion **19** with rare tribromide as the counteranion. In this case no bromination of the *N*-phenyl ring was observed. To the best of our knowl-

edge, this is the first isolation of ionic selenenyl halides and only the second example of stable isolable selenenium cations which are stable under ambient conditions.

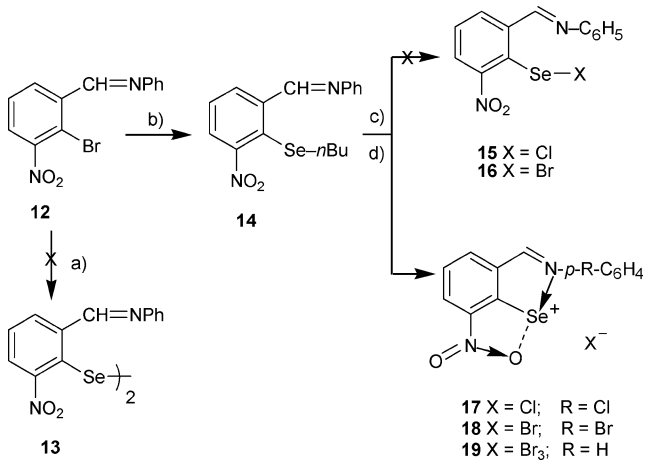

Scheme 2. a) Na_2Se_2, THF, room temp.; b) *n*BuSeNa, C_2H_5OH; c) SO_2Cl_2, Et_3N, $CHCl_3$, 0 °C; d) Br_2, Et_3N, $CHCl_3$, 0 °C.

In an attempt to prepare the corresponding selenenyl sulfide (ArSeSPh), when **19** was treated with thiophenol (PhSH, 2 equiv.), the reaction provided two unexpected products (Scheme 3); cyclic diselenide **20** and novel bicyclic selenide **21** in addition to diphenyl disulfide (38%). Compound **20** was obtained as dark red crystals in very low yield (5%) in comparison to **21** (48%). Compound **21** was isolated as a solvate with dichloromethane during crystallization. There are very few reports concerning the compounds of type **20** and **21**.[17] The sulfur analogue of **21** has been reported in the literature.[17b]

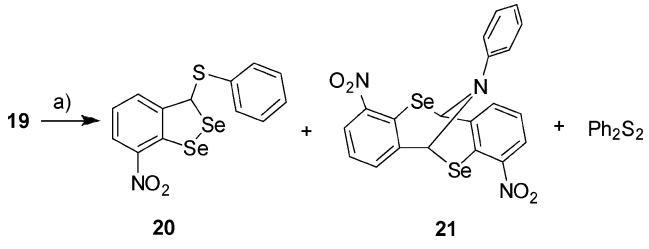

Scheme 3. a) PhSH (2 equiv.), CH_3CN, room temp.

Plausible mechanisms for the formation of **20** and **21** are given in Scheme 4 and Scheme 5. The formation of **20** involves a nucleophilic attack by the PhS^- ion at the electrophilic imine carbon and **21** involves an attack by the nucleophile at selenium in **19**.

The reaction of **18** with an excess of H_2O_2, interestingly, afforded 2-(4-bromophenyl)-7-nitro-1,2-benzisoselenazol-(2*H*)-3-one *Se*-oxide (**22**) in which the Se^{IV} moiety is stabilized by nonbonding Se···O intramolecular interaction with the *ortho*-nitro group (vide infra) (Scheme 6). In the reaction, the imine carbon was oxidized into the carbonyl group and selenium(II) into selenium(IV). It is worth mentioning here that the presence of the nitro group *ortho* to the sele-

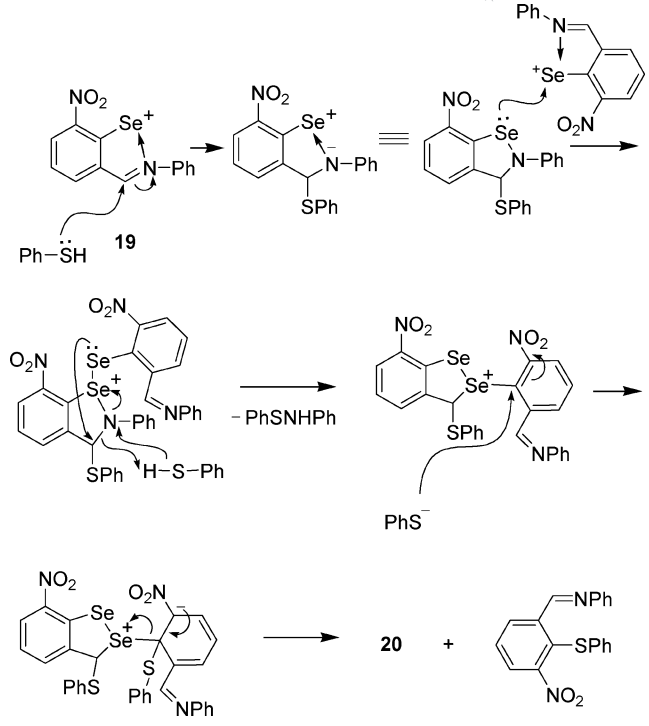

Scheme 4. Formation of **20** by the nucleophilic attack of PhSH at the electrophilic imine carbon.

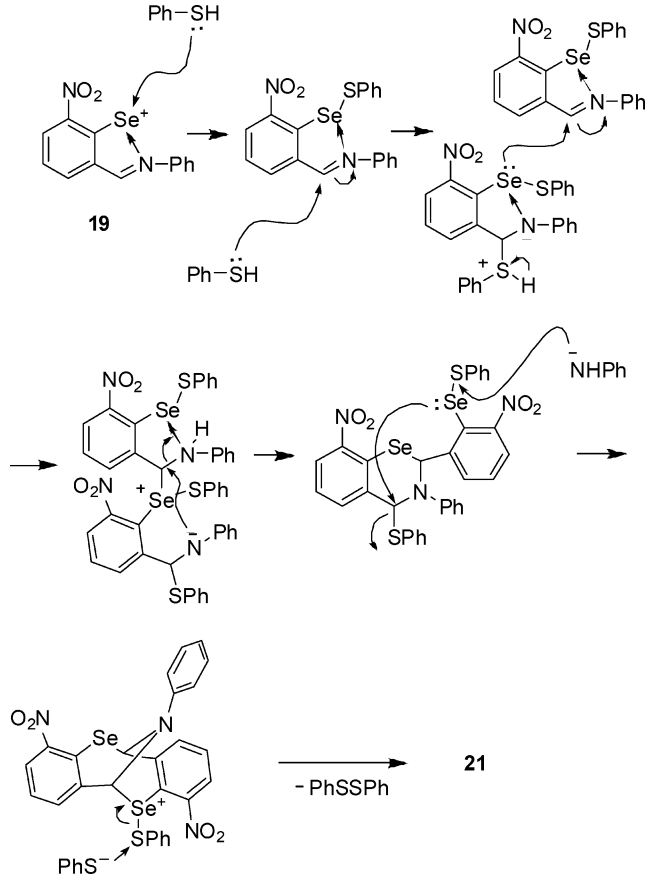

Scheme 5. Formation of **21** by the nucleophilic attack of PhSH at the electrophilic selenium.

nium atom in 7-nitro-2-phenyl-1,2-benzisoselenazol(2*H*)-3-one (**23**) is known to enhance the GPx-like activity (Figure 2).[18a] 7-Nitro-2-phenyl-1,2-benzisoselenazol(2*H*)-3-one *Se*-oxide (**24**) has been isolated and is reported to show high GPx-like activity.[18b] Recent studies have shown that 2-phenyl-1,2-benzisoselenazol(2*H*)-3-one *Se*-oxide (**25**) is the more efficient catalyst in the reduction of hydroperoxide. It has been proposed that **25** is involved as the key intermediate in the catalytic cycle of ebselen at higher concentration of peroxide.[19]

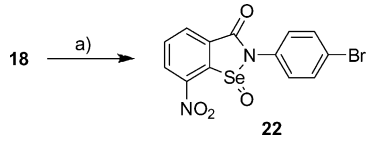

Scheme 6. a) H_2O_2 (30%), CH_3CN, room temp.

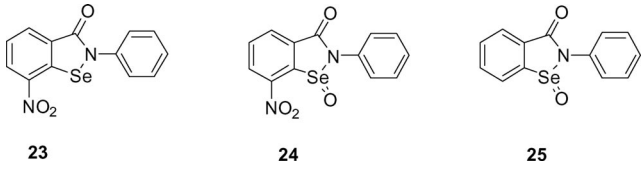

Figure 2. 7-Nitro-2-phenyl-1,2-benzisoselenazol(2*H*)-3-one (**23**) and related selenoxides.

All newly synthesized compounds were fully characterized by ^1H, ^{13}C, ^{77}Se NMR spectroscopy, mass spectrometry techniques and elemental analysis. Some of the compounds were characterized by single-crystal X-ray diffraction studies.

The molecular structure of selenenium ion **18** (Figure 3) indicates a T-shaped geometry around selenium with an N1–Se···O1 bond angle of 155.68(7)°. The Se–N distance [1.895(2) Å] is quite close to the sum of the Pauling covalent radii (1.87 Å) of these two atoms.[20a] The distance is much shorter than the Se–N distance reported for the selenenium cation **5** (2.154 and 2.180 Å).[14a] Also the Se–N distance is less than that reported for aliphatic selenenyl bromides; (1*R*)-2-*endo*-(dimethylamino)methyl-2-*exo*-methoxy-3-*endo*-camphorylselenenyl bromide (Se–N 2.157 Å) and (1*R*)-2-*endo*-(*N*-pyrrolidinyl)methyl-2-*exo*-hydroxy-3-*endo*-camphorylselenenyl bromide (Se–N 2.089 Å).[12j] The Se–Br distance (6.192 Å) in **18** is significantly longer than the sum of the van der Waals radii (3.4 Å).[20b] The Se···O distance [2.544(2) Å] is significantly shorter than the sum of the van der Waals radii (3.4 Å) and indicates a weak Se···O intramolecular interaction within the O–Se–N three-center system with a strong Se–N interaction. Density functional theory studies were carried out at the B3LYP level of theory using the 6-31+G(d) basis set for compound **18**. Natural bond orbital (NBO) analyses were carried out to get an idea of the interaction energy between selenium and oxygen atoms. The NBO second-order perturbation energy for the Se···O1 interaction for **18** is $E_{Se\cdots O}$ = 17.3 kcal mol^{-1} (Table 1). The calculated ^{77}Se NMR chemical shift (1094 ppm) is higher than the experimental value (δ = 937 ppm) (Table 2).

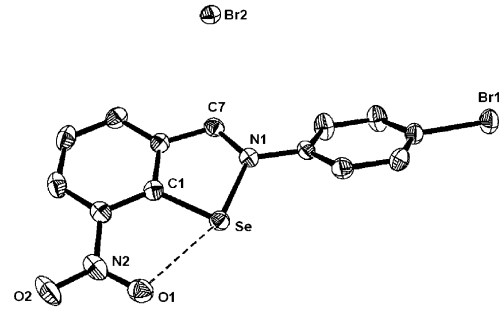

Figure 3. Molecular structure of compound **18**. Thermal ellipsoids are set at 50% probability. Hydrogen atoms are omitted for clarity. Significant bond lengths [Å] and angles [°]: Se–N1 1.895(0); Se···O1 2.544(2); C1–Se–N1 83.86(0); O1···Se–N1 155.68(0).

Table 1. The theoretical data for **17**–**22** obtained by DFT calculations at the B3LYP/6-31+G(d) level along with experimental Se···O distances. Second perturbation energies on **17**–**22** calculated at the B3LYP/6-31+G(d)//6-311+G(d,p) level.

Compound	$r_{Se\cdots O}$ [Å] (calcd.)	$r_{Se\cdots O}$ [Å] (exp.)	$E_{Se\cdots O}$ [kcal mol^{-1}]
17	2.690	–	19.21
18	2.532	2.544	17.3
19	2.445	2.522	21.3
20	2.527	2.593	14.8
21	2.654 [Se1···O1A]	2.711	8.99
	2.615 [Se2···O1B]	2.623	10.07
22	2.757	2.749	5.83

Table 2. Summary of DFT calculations on **17**–**22** at the B3LYP/6-31+G(d) level. NBO analysis and GIAO ^{77}Se NMR chemical shifts calculated in the gas phase at the B3LYP/6-311+G(d,p) level using the *Gaussian 03* suite of quantum chemical calculations along with experimental ^{77}Se NMR chemical shifts.

Compound	q_{Se}	q_O	^{77}Se (calcd.)[a]	^{77}Se (exp.)[a]
17	+0.886	–0.369	1371	1185
18	+0.776	–0.406	1094	937
19	+0.840	–0.417	1118	1185
20	+0.407	–0.395	613, 642	489, 430
21	+0.462	–0.383	431	410
	+0.527	–0.388	–	–
22	+1.579	–0.381	1118	1181

[a] These values are referenced with respect to Me_2Se. Compounds **18**–**22** were optimized on the basis of their known crystal structures.

The molecular structure of **19** (Figure 4) is quite similar to **18** except for the counter anion tribromide (Br_3^-) which has inequivalent bond lengths (Br3–Br2 2.593 Å, Br2–Br1 2.489 Å), and angle Br3–Br2–Br1 176.3°. The coordination geometry around selenium is T-shaped with a N1–Se···O1 bond angle of 156.87(0)°. It is worth noting that the NBO second-order perturbation energy for the Se···O interaction ($E_{Se\cdots O}$ = 21.3 kcal mol^{-1}) is higher than that for **18** ($E_{Se\cdots O}$ = 17.3 kcal mol^{-1}) and suggests a stronger Se···O interaction in this case (Table 2). The calculated ^{77}Se NMR chemical

shift (1118 ppm) is comparable to the experimental value (1185 ppm) which is more downfield than **18**, indicating a higher positive charge on the selenium (vide infra) in **19** (Table 2).

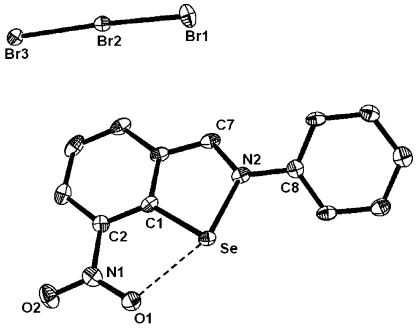

Figure 4. Molecular structure of compound **19**. Thermal ellipsoids are set at 50% probability. Hydrogen atoms are omitted for clarity. Significant bond lengths [Å] and angles [°]: Br3–Br2 2.593(7); Br2–Br1 2.489(7); Se–N2 1.899(2); Se···O1 2.521(3); Br3–Br2–Br1 176.26(0); C1–Se–N2 84.91(0); N2–Se···O1 156.87(0).

The coordination geometry around the Se1 atom in **20** is nearly T-shaped and Se2 is V-shaped (Figure 5). The C1–Se1–Se2–C7 dihedral angle (–20.27°) is quite small indicating a "*cisoid*" conformation.[16g] The Se···O1 distance [2.593(1) Å] is close to that observed in **18** [2.544(1) Å] and **19** [2.521(3) Å]. The NBO second-order perturbation energy for the Se···O interaction ($E_{Se\cdots O}$ = 14.8 kcal mol^{-1}) is smaller than for **18** and **19** indicating a weaker Se···O interaction (Table 1). The calculated ^{77}Se NMR chemical shifts are comparable to the experimental values (Table 2).

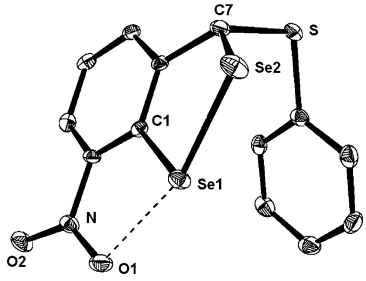

Figure 5. Molecular structure of compound **20**. Thermal ellipsoids are set at 50% probability. Hydrogen atoms are omitted for clarity. Significant bond lengths [Å] and angles [°]: Se1–Se2 2.363(0); Se1···O1 2.593(1); Se2–Se1–C1 90.01(0); Se1–Se2–C7 92.05(0); Se2–Se1···O1 161.94(0).

The coordination geometry around selenium atoms in **21** is also T-shaped with each selenium atom bonded to a carbon atom of phenyl rings, carbon atoms of the bicyclic ring and oxygen atoms of the nitro groups (Figure 6). Intramolecular distances between selenium atoms and the nitro group oxygen atoms (Se1···O1A 2.711 Å; Se2···O1B 2.623 Å) are shorter than the sum of the van der Waals radii (3.4 Å). The NBO second-order perturbation energies for the Se···O interactions ($E_{Se1\cdots O1A}$ = 8.99 kcal mol^{-1}, $E_{Se2\cdots O1B}$ = 10.07 kcal mol^{-1}) are in line with the Se···O distances observed in **18**, **19**, and **20**.

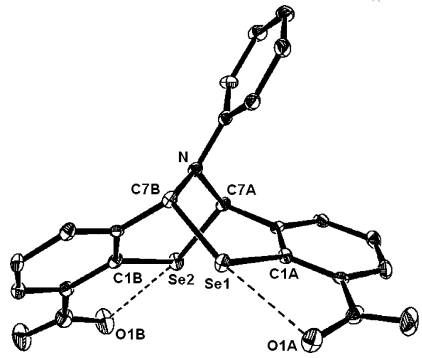

Figure 6. Molecular structure of compound **21**. Thermal ellipsoids are set at 50% probability. Hydrogen atoms and dichloromethane molecule omitted for clarity. Significant bond lengths [Å] and angles [°]: Se1–C1A 1.898(1); Se1–C7B 2.046(2); Se2–C1B 1.898(0); Se2–C7A 1.991(2); Se1···O1A 2.711(3); Se2···O1B 2.623(3); C7B–Se1–C1A 99.15(0); C7A–Se2–C1B 100.74(0); C7B–Se1···O1A 170.04(0); C7A–Se2···O1B 170.41(0).

The molecular structure of **22** (Figure 7), shows a see-saw geometry around selenium with a N1–Se···O2 bond angle of 151.74°. The Se–N distance [1.888(2) Å] is similar to that reported for **23** [1.896(3) Å].[21] The Se=O1 bond length [1.638(0) Å] is also close to that reported for a typical seleninate ester (1.630 Å).[16g] The Se···O2 distance [2.749(6) Å] is greater than that in **23** [2.573(3) Å], however, significantly shorter than the sum of the van der Waals radii (3.4 Å). This indicates a weak Se···O intramolecular interaction in comparison to **17**–**21**. The NBO second-order perturbation energy for the Se···O interaction ($E_{Se\cdots O}$ = 5.83 kcal mol^{-1}) is smaller than that for **18** and **19**.

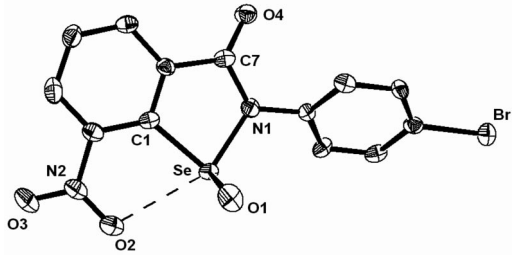

Figure 7. Molecular structure of compound **22**. Thermal ellipsoids are set at 50% probability. Hydrogen atoms and dichloromethane molecule omitted for clarity. Significant bond lengths [Å] and angles [°]: Se–C1 1.953(9); Se–N1 1.888(8); Se–O1 1.638(6); Se···O2 2.749; C1–Se–N1 83.7(3); N1–Se–O1 102.8(3); N1–Se···O2 151.74(0).

To gain better insight into the mechanism of ionization and isolation of the stable selenenium cations, selenenyl bromide **26**[16f] containing only one coordinating imine was optimized (Figure 8).

The calculated Se···N (2.184 Å) and Se–Br distances (2.526 Å) are close to those observed experimentally and, in particular, the Se–Br distance is longer than the sum of the covalent radii (2.31 Å), which indicates a bond lengthening (Table 3). The significant bond elongation of the Se–Br bond is due to the strong Se···N interaction. A significant extension of the Se–I (2.777 Å) bond has also been

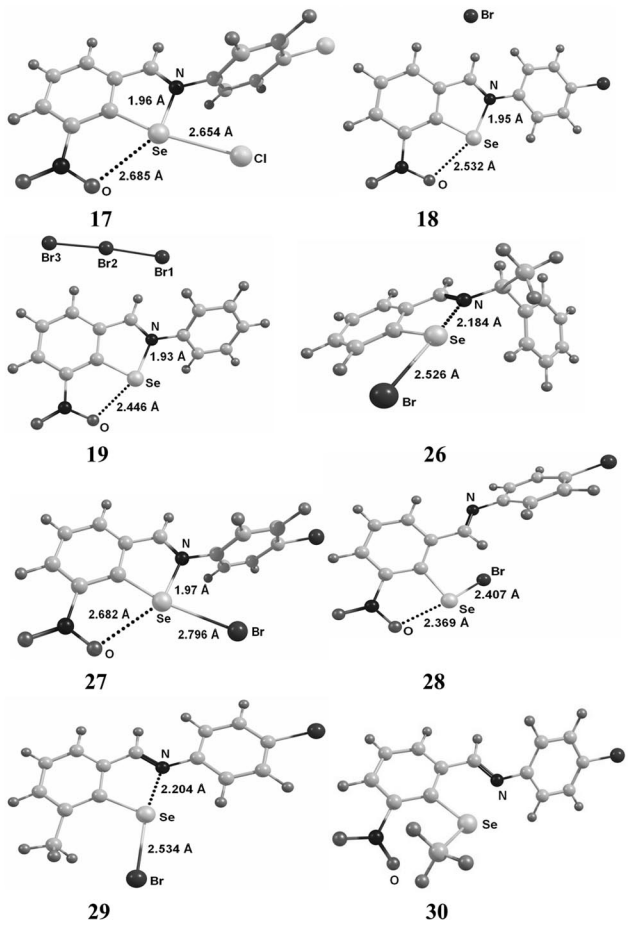

Figure 8. Optimized geometries of **17**–**19** and **26**–**30**. The optimizations of the geometries were performed at the B3LYP/6-31+G(d) level of theory.

observed in [2-(4,4-dimethyl-2-oxazolinyl)phenyl]selenenyl iodide.[16a] To delineate the role of the second coordinating group, selenenyl bromide **27** was optimized (Figure 8). The optimized geometry of **27** exhibits Se–N/Se···O interactions. The Se–N (1.970 Å) and Se···O (2.682 Å) distances are close to the experimentally observed values. The Se–Br distance (2.795 Å) is significantly elongated and indicates the formation of a contact ion pair in the gas phase (Table 3).

Table 3. The theoretical data for **26**–**30** obtained by DFT calculations at the B3LYP/6-31+G(d) level and NBO analysis calculated at the B3LYP/6-31+G(d)//6-311+G(d,p) level.

Compound	q_{Se}	Se···O [Å]	Se–N [Å]	Se–Br [Å]
26	+0.547	–	2.184	2.526
27	+0.846	2.682	1.97	2.796
28	+0.514	2.369	4.545	2.407
29	+0.525	–	2.204	2.534
30	+0.496	3.208	2.775	–

To further establish the role of the positive charge on selenium during the ionization of the Se–Br bond, the NBO charges were calculated. It is worth mentioning that the high positive charge on the selenium is influenced by both the electronegative group bonded to the selenium and the intramolecular interaction. It is well established that strong intramolecular coordination between Se–N/Se···O leads to a significant downfield shift in ^{77}Se NMR[3m,22] and thus, it enhances the positive charge on selenium. The NBO charge on selenium in the case of **27** was found to be +0.846 which is significantly greater than +0.547, observed for **26** (Table 3). This clearly establishes the role of the second coordinating group in enhancing the positive charge on selenium and inducing the ionization of the Se–Br bond. It appears that the strong coordination of the imine nitrogen plays a crucial role in the ionization.

When optimization was carried out for **28** with the imine nitrogen pointing away from selenium and only with nitro group coordination, the Se–Br distance was found to be 2.407 Å, indicating no significant bond elongation. Also the NBO charge on the selenium was found to be +0.514. In another experiment, when the nitro group was replaced with a CH_3 group in **29**, the resulting optimized geometry was found to be very similar to **26** which, has only one imine coordinating group. To establish the role of the electronegativity of bromine in enhancing the positive charge on selenium, bromine was replaced with a CH_3 group in **30**. Interestingly, in this case both the coordinating groups were pointing away from the selenium and the charge on selenium was found to be +0.496 (Table 3). Finally, DFT calculations were done on the crystal structures of **18** and **19**. Selenenium ion **18** exhibits Se–N/Se···O distances similar to those observed in the gas phase. Surprisingly, the bromide ion was found several angstroms away from selenium in **18** as compared to **27**. This may be due to packing effects in the solid state. Compound **19** exhibits more charge on selenium (+0.840) than **18** (+0.775). In the case of **17**, the charge on the selenium was found to be highest in the series (Table 2). The high charge on selenium in **17** is due to the difference in the electronegativity of chlorine and bromine. The optimized geometry of **17** is similar to **27** except for the difference in counter anions (Figure 8). The NBO second-order perturbation energy for the Se···O interaction indicates a weak interaction. To understand the factors for the unusually high NBO charge on the selenium in **19**, calculations of the nucleus-independent chemical shifts (NICS) were carried out. Surprisingly, the NICS (0) value for the five-membered heterocyclic ring in **19** was found to be –8.0 ppm which is equal to benzene (–8.0 ppm).[23,24] This indicates a significant delocalization of the selenium *p*-electrons leading to a strongly aromatic five-membered heterocycle (Figure 9). The delocalization of *p*-electrons on the selenium is further corroborated by a considerable downfield chemical shift of **19** and the delocalization also facilitates ionization of the Se–Br bond.

The GPx-like activities of the selenenium cations and related derivatives were determined by the reductase coupled assay, using UV/Vis spectrophotometry. The decrease in *β*-nicotinamide adenine dinucleotide phosphate (NADPH) concentration was monitored spectrophotometrically at 340 nm. The initial reduction rates (υ_0) for H_2O_2 by reduced glutathione (GSH) in the presence and absence of catalysts were calculated from a linear fit spanning the first 5–10%

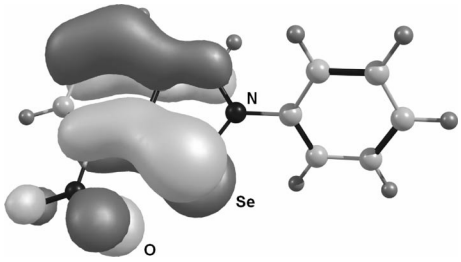

Figure 9. HOMO-11 of **19** showing the delocalization of p electrons in the five-membered heterocycle optimized at B3LYP/6-311+G(d,p). The tribromide ion is omitted for clarity.

of the reaction. It was found that cations **17**, **18**, and **19** were more efficient catalysts in comparison to ebselen (Table 4). Compound **19** is almost 3.5-times more active than ebselen. Cyclic diselenide **20** and selenide **21** showed poor GPx activity. Compound **22** has the highest activity in the series. The higher catalytic activity of **22** is, presumably, due to the presence of a nitro group *ortho* to the selenium atom. It has been reported that the presence of a nitro group *ortho* to the selenium improves the GPx-like activity of seven-substituted ebselen derivatives.[18a]

Table 4. Initial rates, v_0 ($\mu M\,min^{-1}$) for the reduction of H_2O_2 by GSH for **12** and **17**–**22** at 25 °C.

Entry	Compound	v_0 [$\mu M\,min^{-1}$][b]
i	control[a]	15.2 ± 2.0
ii	ebselen	118.2 ± 2.9
iii	**12**	14.9 ± 0.5
iv	**17**	256.7 ± 2.3
v	**18**	270.9 ± 0.6
vi	**19**	404.3 ± 3.4
vii	**20**	46.9 ± 1.4
viii	**21**	24.3 ± 1.3
ix	**22**	472.7 ± 3.5

[a] Control values were obtained from the reduction of H_2O_2 by GSH in the absence of GPx samples. [b] Assay conditions: reactions were carried out with 0.1-M phosphate buffer pH 7.5, with EDTA (1 mM), GSH (2 mM), NADPH (0.4 mM), GR (1.3 unit/mL), selenium compounds (80 μM), and H_2O_2 (1.6 mM).

To further establish that the GPx mimetics were working as catalysts and not undergoing only stoichiometric reactions, we carried out several control experiments in the absence and presence of various components of the bioassay, such as with catalyst and GSH, catalyst and H_2O_2 etc. Since **19** itself reacts with the system [containing GSH and glutathione reductase (GR), data not shown], achieving complete conversion of GSH into oxidized glutathione (GSSG) is difficult to monitor. However, the reaction rates remained linear for at least 5 min. When only compound **19** (10 μM) was added into the mixture [containing 0.1 M buffer pH 7.5, 1 mM ethylenediamine tetraacetate (EDTA), 2 mM GSH, 0.4 mM NADPH, 1 unit of GR], the rate was found to be 1.93 $\mu M\,min^{-1}$ and 9.64 μM of GSSG was formed in 5 min (see Figure S51 in the Supporting Information). Subsequently, when H_2O_2 (1.6 mM) was added into the above reaction mixture, the rate was increased to 6.75 $\mu M\,min^{-1}$ and 33.76 μM of GSSG was formed in 5 min (see Figure S52 in the Supporting information for this article which is available on the WWW under http://dx.doi.org/10.1002/ejic.200900669). For compound **19**, 48.24 μM of GSH was oxidized into GSSG (24.12 μM) at lower catalyst concentration (10 μM). Thus, when compared to the catalyst **19** alone, at least four times more GSH was oxidized in 5 min.

To understand the mechanism and identify the intermediates involved in the catalytic cycle of selenenium cations, detailed ^{77}Se NMR spectroscopy experiments for **19** were carried out. When **19** was treated with H_2O_2 (2 equiv.) in [D_6]DMSO, no new signal except that for **19** at δ = 1183 ppm was observed. On the addition of more H_2O_2 (4 equiv.), a new signal at δ = 1185 ppm was observed and is assigned to selenoxide **24** (Scheme 7). Further addition of H_2O_2 (6 equiv.) did not lead to any change in the ^{77}Se NMR spectrum. The identity of the obtained product **24** was further established by comparing the ^{77}Se NMR chemical shift (1181 ppm) of the closely related **22** prepared from the reaction of **18** with H_2O_2 (6 equiv.). The formation of **24** may take place via seleninic acid **31**. The reaction did not lead to the observation of a ^{77}Se NMR signal around 1300 ppm expected for the formation of **31** at this stage of the reaction. It is worth comparing that ebselen on reaction with H_2O_2 has been reported to exhibit a ^{77}Se NMR signal at δ = 1122 ppm due to the formation of seleninic acid.[19c] However, the addition of PhSH (2 equiv.) to the mixture produced two new signals at 439 and 1372 ppm, respectively. The signal at δ = 439 ppm is assigned to selenenyl sulfide **33**. The signal of **33** is close to that observed for 2,6-diformyl-4-*tert*-butylphenylselenenyl sulfide (δ = 435 ppm).[16c] The signal was completely different from those obtained for **20** (430, 489 ppm) and **21** (δ = 410 ppm) from the reaction of **19** with PhSH (2 equiv.) in acetonitrile at room temperature. The other signal obtained at δ = 1372 ppm is assigned to seleninic acid **31**. The signal of **31** is shifted downfield by 25 ppm from *N*,*N*-dimethylbenzylamineseleninic acid (1347 ppm)[3m] indicating a strong Se···O interaction with the *ortho* nitro group. The formation of selenosulfide **33** probably takes place through thioseleninate **32** for which no ^{77}Se NMR signals were observed. When more PhSH (4 equiv.) was added into the mixture, a new signal at δ = 1191 ppm was observed which is assigned to **24**. The signal is also in the range of peaks expected for selenenic acids, for example: *ortho*-nitrobenzeneselenenic acid (1066)[25] and 2-[(cyclohexyl-methylamino)methyl]benzeneselenenic acid (1173 ppm).[3c] As selenol **34** is a highly reactive species and can be easily oxidized to give back **24** via selenenic acid **35**, we suggest that the signal at δ = 1191 ppm is due to **24** and not due to **35**. Fisher and Dereu[19a] have also proposed that ebselen at higher peroxide concentrations is first oxidized to its selenoxide, which then reacts with PhSH (1 equiv.) to form the corresponding thioseleninate. Alternatively, the formation of thioseleninate **32** may also take place from the reaction of **31** with PhSH. Kice et al.[26] have reported the formation of thioseleninate when benzeneseleninic acid was treated with thiol. On the

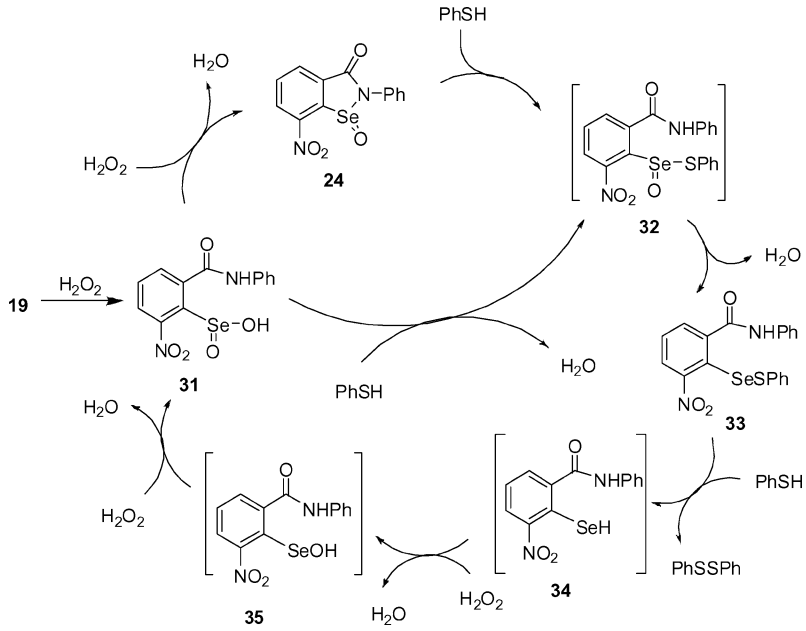

Scheme 7. Proposed catalytic cycle for the reduction of H_2O_2 by **19**.

basis of the above observations, we propose the following catalytic mechanism for the reduction of H_2O_2 with PhSH in the presence of **19**.

Conclusions

We have isolated the first examples of stable ionic selenenyl chloride, bromide, and tribromide. Strong coordination by the imine nitrogen plays an important role in ionization of the Se–halide bond. The Se–N/Se···O interactions by two coordinating groups and the consequent five-membered aromatic heterocycle ring formation lead to a high positive charge on selenium. Both the high positive charge on the selenium and the aromaticity of the five-membered heterocyclic ring facilitate the ionization of the Se–Br bond. The heterocycle is closely related to ebselen and exhibits excellent GPx-like activity probably due to the in situ formation of corresponding selenoxides.

Experimental Section

General Procedure: *n*-Butyllithium, selenium powder, and 3-nitrophthalic acid were purchased from Sigma–Aldrich. All other chemicals were of highest purity available. All reactions were performed under nitrogen or argon by modified Schlenk techniques and monitored by thin-layer chromatography techniques from time to time. All the experiments were carried out in a well-ventilated fume hood. Column chromatography was performed on glass columns loaded with silica gel of 60–120 mesh. Solvents were purified by standard techniques.[27] Melting points were recorded by a VEEGO melting point (VM*P*-1) apparatus and are uncorrected. ^{1}H (399.88 MHz), ^{13}C (100.56 MHz), and ^{77}Se (57.26 MHz) NMR spectra were recorded with a Varian NMR-Mercury plus 400 MHz spectrometer and 300 MHz for ^{77}Se NMR at the indicated frequencies. Chemicals shifts (δ) are shown with respect to $SiMe_4$ (TMS) as internal for nuclei ^{1}H and ^{13}C and Me_2Se as external standards for nuclei ^{77}Se. Data were recorded as follows: chemical shifts, integration multiplicity (s = singlet, d = doublet, t = triplet, m = multiplet), coupling constants (Hz), and assignment. Optical rotation was measured with an Autopole IV Automatic Polarimeter. The mass spectra were recorded at room temperature with a Micro mass Q–TOF (YA 107) mass spectrometer. Elemental analyses were performed with a CHN–CE instruments Flash 1112 series EA Theroquest elemental analyzer. Infrared spectra were recorded in the range 4000–450 cm^{-1} using KBr for solid samples and neat for liquid samples between CsI plates on a Perkin–Elmer spectrum one FT–IR spectrometer. The UV–VIS spectra in solution for GPx activity were recorded with a JASCO, V-570 spectrometer.

Synthesis of 12: To a solution of 2-bromo-3-nitrobenzaldehyde[28] (19.56 mmol, 4.5 g) in glacial acetic acid (30 mL) was added distilled aniline (19.56 mmol, 1.82 g, 2.5 mL) with continuous stirring at room temperature. After completion of the addition of aniline, a yellow precipitate was formed. To complete the precipitation, the reaction mixture was cooled with ice, then filtered and washed with ice-cooled ethanol. Recrystallization from hot ethanol afforded a light yellow solid; yield 3.7 g (83%); m.p. 116–118 °C. ^{1}H NMR ($CDCl_3$): δ = 7.26–7.46 (m, 5 H, ArH), 7.53–7.57 (t, J = 7.32 Hz, 1 H, ArH), 7.79–7.81 (dd, J = 7.93, 1.52 Hz, 1 H, ArH), 8.43–8.46 (dd, J = 7.93, 1.83 Hz, 1 H, ArH), 8.92 (s, 1 H) ppm. ^{13}C NMR ($CDCl_3$): δ = 116.9, 121.3, 126.9, 127.3, 128.3, 129.5, 132.1, 137.3, 150.9, 151.6, 157.5 ppm. IR (KBr): $\tilde{\nu}$ = 3387, 2918, 1614 (C=N), 1586, 1533 (NO_2), 1486, 1362, 1259, 1212, 1034, 810, 762, 739, 699 cm^{-1}. MS (TOF MS ES$^+$): m/z (%) = 305.085 [M + H]$^+$. $C_{13}H_9BrN_2O_2$ (305.13): calcd. C 51.17, H 2.97, N 9.18; found C 51.45, H 2.60, N 9.09.

Synthesis of 14: To a solution of di-*n*-butyl diselenide (1.2 mmol, 0.34 g) in deoxygenated ethanol (10 mL), was added $NaBH_4$ (2.2 mmol, 0.08 g) at 0 °C under an inert atmosphere. The reaction mixture was stirred at room temperature for 30 min. Compound **12** (2.0 mmol, 0.61 g) was added to the in situ prepared *n*BuSeNa at 0 °C. The reaction mixture was stirred at room temperature for 2 h. The excess of solvent was removed under vacuum. The residue was dissolved in chloroform and washed with water. The organic layer and the chloroform extracts from the aqueous layer were combined

and dried with anhydrous sodium sulfate. Removal of solvent and purification of the residue by silica gel column chromatography (elution with 4% ethyl acetate/petroleum ether) afforded an orange liquid. IR (neat): $\tilde{\nu}$ = 2959, 1619 (C=N), 1532 (NO_2), 1363 cm^{-1}. HRMS (Q-TOF MS): *m*/*z* calcd. for $C_{17}H_{18}O_2N_2Se$ [M + H]$^+$: 363.0619; found 363.0612. ^{77}Se NMR ($CDCl_3$): δ = 212 ppm.

Synthesis of 17: To a solution of compound **14** (1.05 mmol, 0.38 g) in $CHCl_3$ (5 mL) was added SO_2Cl_2 (2.1 mmol, 0.28 g, 0.168 mL) in $CHCl_3$ (2 mL) in the presence of Et_3N (2.1 mmol, 0.21 g, 0.27 mL) at 0 °C with continuous stirring under an inert atmosphere. Additionally, the reaction mixture was stirred at room temperature for 30 min. The resulting greenish-yellow precipitate was filtered off and dried under vacuum. Recrystallization from MeOH afforded a green solid; yield 0.18 g (45%); m.p. 193–195 °C. ^{1}H NMR (CD_3OD): δ = 7.75–7.99 (m, 4 H, ArH), 8.20–8.24 (t, *J* = 7.94 Hz, 1 H, ArH), 8.98–9.01 (dd, *J* = 8.24, 0.91 Hz, 1 H, ArH), 9.05–9.07 (dd, *J* = 7.99, 1.91 Hz, 1 H, ArH), 10.61 (s, 1 H) ppm. ^{13}C NMR (CD_3OD): δ = 124.7, 131.2, 131.9, 132.0, 133.4, 135.5, 140.1, 140.8, 144.1, 146.8, 164.89 ppm. IR (KBr): $\tilde{\nu}$ = 2894, 1613 (C=N), 1519 (NO_2), 1414, 1313, 766 cm^{-1}. MS (TOF MS ES$^+$): *m*/*z* (%) = 304.9208 ([M – 2Cl]$^+$, ^{80}Se, 100%). ^{77}Se NMR (CD_3OD): δ = 1185 ppm. $C_{13}H_8Cl_2N_2O_2Se$ (374.08): calcd. C 41.74, H 2.16, N 7.49; found C 42.06, H 2.71, N 7.43.

Synthesis of 18: To a solution of compound **14** (0.62 mmol, 0.23 g) in $CHCl_3$ (5 mL) was added Br_2 (0.62 mmol, 0.11 g, 0.04 mL) in $CHCl_3$ (2 mL) in the presence of Et_3N (1.24 mmol, 0.13 g, 0.17 mL) at 0 °C with continuous stirring under an inert atmosphere. After the complete addition of Br_2, the reaction mixture was stirred at room temperature for 2 h. The yellow precipitate was filtered off and dried under vacuum. Recrystallization from DMSO/MeOH afforded red crystals of **18**; yield 0.16 g (55%); m.p. 244–246 °C. ^{1}H NMR ([D$_6$]DMSO): δ = 7.76–7.79 (m, 4 H, ArH), 8.20–8.24 (t, *J* = 8.24 Hz, 1 H, ArH), 8.99–9.01 (dd, *J* = 7.99, 0.91 Hz, 1 H, ArH), 9.02–9.08 (dd, *J* = 7.93, 0.91 Hz, 1 H, ArH), 10.60 (s, 1 H) ppm. ^{13}C NMR ([D$_6$]DMSO): δ = 123.6, 130.4, 130.6, 130.7, 131.9, 133.8, 139.1, 139.2, 142.5, 145.0, 162.6 ppm. IR (KBr): $\tilde{\nu}$ = 3016, 2928, 1611 (C=N), 1577, 1516 (NO_2), 1413, 1356, 1308, 1075, 1005, 820, 809, 733 cm^{-1}. MS (TOF MS ES$^+$): *m*/*z* (%) = 382.73 ([M – Br]$^+$, ^{80}Se, 100%). ^{77}Se NMR ([D$_6$]DMSO): δ = 937 ppm. $C_{13}H_8Br_2N_2O_2Se$ (462.99): calcd. C 33.72, H 1.74, N 6.04; found C 33.66, H 1.55, N 6.55.

Synthesis of 19: To a solution of compound **14** (0.44 mmol, 0.16 g) in chloroform (5 mL) was added Br_2 (0.88 mmol, 0.14 g, 0.06 mL) in $CHCl_3$ (2 mL) in the presence of Et_3N (0.88 mmol, 0.088 g, 0.12 mL) at 0 °C with continuous stirring under an inert atmosphere. Additionally, the reaction mixture was stirred at room temperature for 40 min. The resulting red precipitate was filtered off after which it turned into a yellow precipitate. The crude product was recrystallized from diethyl ether/CH_3CN/CH_2Cl_2 to give light yellow crystals; yield 0.06 g (60%); m.p. 175–178 °C. ^{1}H NMR (CD_3CN): δ = 7.73–7.87 (m, 5 H, ArH), 8.15–8.19 (t, *J* = 7.93 Hz, 1 H, ArH), 8.88–8.90 (dd, *J* = 7.99, 0.91 Hz, 1 H, ArH), 9.00–9.03 (dd, *J* = 7.99, 0.91 Hz, 1 H, ArH), 10.19 (s, 1 H) ppm. ^{13}C NMR (CD_3CN): δ = 125.2, 132.1, 132.5, 132.6, 134.0, 135.4, 140.6, 140.7, 144.3, 147.0, 162.8 ppm. IR (KBr): $\tilde{\nu}$ = 3032, 2992, 2920, 2855, 1614 (C=N), 1561, 1526 (NO_2), 1451, 1413, 1360, 1300, 1231, 1005, 804 759, 732 cm^{-1}. MS (TOF MS ES$^+$): *m*/*z* (%) = 304.87 (M$^+$, ^{80}Se, 100%). ^{77}Se NMR (CD_3CN): δ = 1185 ppm. $C_{13}H_9Br_3N_2O_2Se$ (543.91): calcd. C 28.71, H 1.67, N 5.15; found C 28.26, H 1.41, N 5.99.

Synthesis of 20: Benzenethiol (4 mmol, 0.41 mL) was added to a solution of compound **19** (2 mmol, 1.05 g) in acetonitrile (10 mL). The mixture was stirred at room temperature for 5 h, concentrated under vacuum, and the oily liquid was dissolved in water (10 mL). The aqueous layer was extracted with chloroform. The separated organic layers were dried with anhydrous sodium sulfate. Removal of solvent and purification of the residue by silica gel column chromatography (elution with 5% ethyl acetate/petroleum ether) afforded two products **20** and **21**, respectively. Recrystallization of **20** from CH_2Cl_2/petroleum ether (1:1) gave red crystals; yield 0.045 g (5%); m.p. 135 °C. ^{1}H NMR ($CDCl_3$): δ = 6.20 (s, 1 H), 7.27–7.40 (m, 7 H, ArH), 8.16–8.18 (t, *J* = 7.27 Hz, 1 H, ArH) ppm. ^{13}C NMR ($CDCl_3$): δ = 59.2, 125.1, 126.6, 129.1, 129.3, 129.4, 132.4, 133.2, 134.8, 139.6, 146.7 ppm. IR (KBr): $\tilde{\nu}$ = 3442, 2923, 2851, 1588, 1512 (NO_2), 1324, 1295, 749, 720 cm^{-1}. MS (TOF MS ES$^+$): *m*/*z* (%) = 293.72 [M – SC_6H_5]$^+$. ^{77}Se NMR ($CDCl_3$): δ = 430, 489 ppm. $C_{13}H_9NO_2SSe_2$ (401.19): calcd. C 38.39, H 2.26, N 3.49, S 7.99; found C 39.01, H 1.97, N 4.18, S 7.91.

Synthesis of 21: Recrystallization of **21** from CH_2Cl_2/petroleum ether (1:1) gave dark red crystals; yield 0.26 g (48%); m.p. 244–246 °C. $[\alpha]_D^{25}$ = –0.002 (*c* = 0.066, $CHCl_3$). ^{1}H NMR ($CDCl_3$): δ = 6.33 (s, 2 H), 7.27–7.01 (m, 5 H, ArH), 7.31–7.34 (t, *J* = 7.63 Hz, 2 H, ArH), 7.53–7.55 (dd, *J* = 8.24, 1.22 Hz, 2 H, ArH), 8.24–8.27 (dd, *J* = 8.24, 1.22 Hz, 2 H, ArH) ppm. ^{13}C NMR ($CDCl_3$): δ = 58.7, 58.9, 119.3, 125.2, 126.1, 126.3, 129.9, 131.8, 132.3, 138.1, 146.0, 146.7 ppm. IR (KBr): $\tilde{\nu}$ = 3076, 2923, 2851, 1597, 1516 (NO_2), 1328, 1264, 1036, 932, 803, 755 cm^{-1}. MS (TOF MS ES$^+$): *m*/*z* (%) = 520.00 ([M + H]$^+$, ^{80}Se, 100%). ^{77}Se NMR ($CDCl_3$): δ = 410 ppm. $C_{20.5}H_{13.5}ClN_3O_4Se_2$ (559.21): calcd. C 44.03, H 2.43, N 7.51; found C 43.42, H 2.15, N 7.95.

Synthesis of 22: To a solution of compound **18** (1.0 mmol, 0.462 g) in acetonitrile (5 mL) was added 30% H_2O_2 (6 mmol, 0.68 mL) at room temperature. The mixture was stirred at room temperature for 1/2 h. The precipitate was filtered off and dried under vacuum to give an orange compound. Recrystallization from DMSO/MeOH/ether gave needle-shaped yellow crystals; yield 0.165 g (40%); m.p. 220–222 °C. ^{1}H NMR ([D$_6$]DMSO): δ = 7.45–7.47 (d, *J* = 8.70 Hz, 2 H, ArH), 7.70–7.72 (d, *J* = 8.70 Hz, 2 H, ArH), 8.14–8.18 (t, *J* = 7.59 Hz, 1 H, ArH), 8.44–8.47 (dd, *J* = 7.59, 1.19 Hz, 1 H, ArH), 8.72–8.75 (dd, *J* = 8.39, 1.19 Hz, 1 H, ArH) ppm. ^{13}C NMR ([D$_6$]DMSO): δ = 120.6, 128.5, 129.1, 132.4, 132.6, 134.4, 135.0, 135.4, 141.9, 143.2, 165.2 ppm. IR (KBr): $\tilde{\nu}$ = 3076, 2933, 1689 (C=O), 1529 (NO_2), 1485, 1340, 1320, 1071, 864 (Se=O), 729 cm^{-1}. MS (TOF MS ES$^+$): *m*/*z* (%) = 414.82 [M + H]$^+$. ^{77}Se NMR ($CDCl_3$): δ = 1181 ppm. $C_{13}H_7BrN_2O_4Se$ (414.08): calcd. C 37.71, H 1.70, N 6.77; found C 37.49, H 1.50, N 7.29.

Reductase-Coupled Assay: The GPx-like activity of organoselenium compounds was determined by the spectrophotometric method at 340 nm described by Wilson et al.[3a] A typical test mixture contained GSH (2 mM), EDTA (1 mM), glutathione reductase (1.3 unit/mL), and NADPH (0.4 mM) in 0.1 M potassium phosphate buffer, pH 7.5. The catalysts (2 mM) were added to the test mixture at 25 °C and the reaction was started by the addition of H_2O_2 (1.6 mM). The initial reduction rates were calculated from the oxidation rate of NADPH at 340 nm. The initial reduction rate was determined at least 3–4 times and calculated from the first 5–10% of the reaction by using 6.22 mM^{-1} cm^{-1} as the extinction coefficient for NADPH.

Computational Studies: All the theoretical calculations were executed by the Gaussian 03 suite of quantum chemical programs.[29] The hybrid Becke 3-Lee–Yang–Parr (B3LYP) exchange correlation functional was implemented for DFT calculations.[30] The geometry optimizations were carried out at the B3LYP level of DFT by using the 6-31+G(d) basis sets. The ^{77}Se NMR calculations were per-

formed at B3LYP/6-311+G (d,p) level on B3LYP/6-31+G(d)-level-optimized geometries by using the gauge-including atomic orbital (GIAO) method (referenced with respect to the peak of Me_2Se).[31] The quantifications of orbital interaction were done by natural bond orbital (NBO) analysis at B3LYP/6-311+G(d,p) level.[32] Nucleus-independent chemical shifts (NICS)[33] were carried out at B3LYP/6-31+G(d)//6-311+G(d,p) level.

X-ray Crystallographic Analysis: The X-ray crystallographic studies were carried out with a CrysAlis CCD diffractometer using graphite-monochromatized Mo-K_α radiation (λ = 0.71073 Å) and data were collected at room temperature (293 K) and 200 K. The structures were solved by direct methods and refined by a full-matrix least-squares procedure on F^2 for all reflections in SHELXL-97 software.[34]

CCDC-726577 (for **18**), CCDC-726578 (for **19**), CCDC-726579 (for **20**), CCDC-726580 (for **21**), and CCDC-734677 (for **22**) contain the supplementary crystallographic data for this paper. These data can be obtained free of charge from The Cambridge Crystallographic Data Centre via www.ccdc.cam.ac.uk/data_request/cif.

Crystal Data for 18: $C_{13}H_8Br_2N_2O_2Se$, Mr = 462.99, monoclinic, space group $P12_1/n1$, a = 12.3695(3) Å, b = 9.0232(2) Å, c = 13.2943(3) Å, $\alpha = \gamma$ = 90°, β = 109.791(3)°, V = 1396.16(6) Å^3, Z = 4, T = 200(2) K, $\rho_{calcd.}$ = 2.203 Mg m^{-3}, GOF = 0.867, R_1 = 0.0331, wR_2 = 0.0542 [$I>2\sigma(I)$]; R_1 = 0.0849, wR_2 = 0.0599 (all data). Of the 20866 reflections that were collected, 5726 were unique (R_{int} = 0.0511).

Crystal Data for 19: $C_{13}H_9Br_3N_2O_2Se$, Mr = 543.91, triclinic, space group $P\bar{1}$, a = 6.9018(3) Å, b = 9.9121(4) Å, c = 12.0342(5) Å, α = 104.843(4)°, β = 95.362(4)°, γ = 99.326(4)°, V = 777.138(6) Å^3, Z = 2, T = 110(2) K, $\rho_{calcd.}$ = 2.324 Mg m^{-3}, GOF = 0.956, R_1 = 0.0422, wR_2 = 0.0908 [$I>2\sigma(I)$]; R_1 = 0.0677, wR_2 = 0.0964 (all data). Of the 9148 reflections that were collected, 5074 were unique (R_{int} = 0.0394).

Crystal Data for 20: $C_{13}H_9NO_2SSe_2$, Mr = 401.19, monoclinic, space group $P12_1/c1$, a = 14.6256(5) Å, b = 12.9422(10) Å, c = 7.1523(2) Å, $\alpha = \gamma$ = 90°, β = 101.816(3)°, V = 1325.15(12) Å^3, Z = 4, T = 110(2) K, $\rho_{calcd.}$ = 2.011 Mg m^{-3}, GOF = 0.947, R_1 = 0.0282, wR_2 = 0.0521 [$I>2\sigma(I)$]; R_1 = 0.0473, wR_2 = 0.0540 (all data). Of the 9693 reflections that were collected, 4374 were unique (R_{int} = 0.0307).

Crystal Data for 21: $C_{20.50}H_{13.50}ClN_3O_4Se_2$, Mr = 559.21, monoclinic, space group $C12_1/c1$, a = 9.3147(4) Å, b = 13.6971(4) Å, c = 31.4352(10) Å, $\alpha = \gamma$ = 90°, β = 91.111(3)°, V = 4009.9(2) Å^3, Z = 8, T = 373(2) K, $\rho_{calcd.}$ = 1.853 Mg m^{-3}, GOF = 1.192, R_1 = 0.0705, wR_2 = 0.1205 [$I>2\sigma(I)$]; R_1 = 0.0913, wR_2 = 0.1247 (all data). Of the 15622 reflections that were collected, 6601 were unique (R_{int} = 0.0360).

Crystal Data for 22: $C_{13}H_7BrN_2O_4Se$, Mr = 414.08, monoclinic, space group $P2_1/n$, a = 13.5497(9) Å, b = 4.2684(2) Å, c = 23.0580(17) Å, $\alpha = \gamma$ = 90°, β = 91.789(7)°, V = 1332.92(15) Å^3, Z = 4, T = 110(2) K, $\rho_{calcd.}$ = 2.063 Mg m^{-3}, GOF = 1.153, R_1 = 0.1031, wR_2 = 0.2491 [$I>2\sigma(I)$]; R_1 = 0.1288, wR_2 = 0.2612 (all data). Of the 8327 reflections that were collected, 4273 were unique (R_{int} = 0.0793).

Supporting Information (see also the footnote on the first page of this article): Details of ^{1}H NMR, ^{13}C NMR, MS, IR spectra and elemental analysis data of all newly synthesized compounds, ^{77}Se NMR spectra for **14** and **17**–**22**, ^{77}Se NMR spectra of catalytic cycle for **19**, tables of coordinates, NBO charges, NBO second-order perturbation energies, for all optimized geometries **17**–**22** and **26**–**30**, NICS calculations for **17**–**20** and for GPx-like activity of **12** and **17**–**22**.

Acknowledgments

We are grateful to the Department of Science and Technology (DST), New Delhi, for the award of the Ramanna fellowship and the Sophisticated Analytical Instrument Facility (SAIF), Indian Institute of Technology (IIT), Bombay, for recording ^{77}Se NMR spectra. V. P. S. wishes to thank IIT Bombay for a teaching assistantship. We express appreciation to Prof. I. N. N. Namboothiri and Prof. N. S. Punekar for helpful discussions.

[1] a) *Organoselenium Chemistry: A Practical Approach* (Ed.: T. G. Back), Oxford University Press, Oxford, **1999**, pp. 35–66; b) *Organoselenium Chemistry: Modern Development in Organic Synthesis* (Ed.: T. Wirth), *Top. Curr. Chem.*, Springer, Berlin, **2000**, vol. 208.

[2] Reviews: a) T. Wirth, *Angew. Chem.* **2000**, *112*, 3890–3900; T. Wirth, *Angew. Chem. Int. Ed.* **2000**, *39*, 3740–3749; b) D. M. Browne, T. Wirth, *Curr. Org. Chem.* **2006**, *10*, 1893–1903; c) D. M. Freudendanl, S. A. Shahzad, T. Wirth, *Eur. J. Org. Chem.* **2009**, 1649–1664.

[3] a) S. R. Wilson, P. A. Zucker, R.-R. C. Huang, A. Spector, *J. Am. Chem. Soc.* **1989**, *111*, 5936–5939; b) A. Spector, S. R. Wilson, P. A. Zucker, U. S. Patent 5, 321, 138 (C1, 546–224; C07C37/02), **1994**; *Chem. Abstr.* **1994**, *121*, P256039r; c) M. Iwaoka, S. Tomoda, *J. Am. Chem. Soc.* **1994**, *116*, 2557–2561; d) T. Wirth, *Molecules* **1998**, *3*, 164–166; e) G. Mugesh, A. Panda, H. B. Singh, N. S. Punekar, R. J. Butcher, *Chem. Commun.* **1998**, 2227–2228; f) G. Mugesh, H. B. Singh, *Chem. Soc. Rev.* **2000**, *29*, 347–357; g) G. Mugesh, A. Panda, H. B. Singh, N. S. Punekar, R. J. Butcher, *J. Am. Chem. Soc.* **2001**, *123*, 839–850; h) G. Mugesh, W.-W. du Mont, H. Sies, *Chem. Rev.* **2001**, *101*, 2125–2179; i) G. Mugesh, W.-W. du Mont, *Chem. Eur. J.* **2001**, *7*, 1365–1370; j) B. K. Sharma, G. Mugesh, *J. Am. Chem. Soc.* **2005**, *127*, 11477–11485; k) B. K. Sharma, G. Mugesh, *Inorg. Chem.* **2006**, *45*, 5307–5314; l) K. P. Bhabak, G. Mugesh, *Chem. Eur. J.* **2008**, *14*, 8640–8651; m) B. K. Sharma, G. Mugesh, *Org. Biomol. Chem.* **2008**, *6*, 965–974.

[4] a) A. Müller, E. Cadenas, P. Graf, H. Sies, *Biochem. Pharmacol.* **1984**, *33*, 3235–3239; b) A. Wendel, M. Fausel, H. Safayhi, G. Tiegs, R. Otter, *Biochem. Pharmacol.* **1984**, *33*, 3241–3245; c) M. J. Parnham, S. Kindt, *Biochem. Pharmacol.* **1984**, *33*, 3247–3250; d) A. Müller, H. Gabriel, H. Sies, *Biochem. Pharmacol.* **1985**, *34*, 1185–1189; e) H. Safayhi, G. Tiegs, A. Wendel, *Biochem. Pharmacol.* **1985**, *34*, 2691–2694; f) A. Wendel, European Patent 0-165-534, **1985**; g) A. Wendel, G. Tiegs, *Biochem. Pharmacol.* **1986**, *35*, 2115–2118; h) T. Schewe, *Gen. Pharmacol.* **1995**, *26*, 1153–1169; i) M. J. Parnham, H. Sies, *Expert Opin. Invest. Drugs* **2000**, *9*, 607–619.

[5] a) P. V. Jacquemin, L. E. Christiaens, M. J. Renson, M. J. Evers, N. Dereu, *Tetrahedron Lett.* **1992**, *33*, 3863–3866; b) J. Chaudie′re, J.-C. Yadan, I. Erdelmeier, C. Tailhan-Lomount, M. Moutet in *Oxidative Processes and Antioxidants* (Ed.: R. Paoletti), Raven Press, New York, **1994**, pp. 165–184; c) J. Chaudie′re, M. Moutet, P. d'Alessio, *C. R. Soc. Biol.* **1995**, *189*, 861–882; d) I. Erdelmeier, C. Tailhan-Lomount, J.-C. Yadan, *J. Org. Chem.* **2000**, *65*, 8152–8157.

[6] V. Galet, J.-L. Bernier, J.-P. Hénichart, D. Lesieur, C. Abadie, L. Rochette, A. Lindenbaum, J. Chalas, J.-F. Renaud de la Faverie, B. Pfeiffer, P. Renard, *J. Med. Chem.* **1994**, *37*, 2903–2911.

[7] a) H. J. Riech, C. P. Jasperse, *J. Am. Chem. Soc.* **1987**, *109*, 5549–5551; b) T. G. Back, B. P. Dyck, *J. Am. Chem. Soc.* **1997**, *119*, 2079–2083.

[8] a) Z.-P. Wu, D. Hilvert, *J. Am. Chem. Soc.* **1989**, *111*, 4513–4514; b) Z.-P. Wu, D. Hilvert, *J. Am. Chem. Soc.* **1990**, *112*, 5647–5648.

[9] L. Engman, D. Stern, I. A. Cotgreave, C. M. Andersson, *J. Am. Chem. Soc.* **1992**, *114*, 9737–9739.
[10] a) T. G. Back, Z. Moussa, *J. Am. Chem. Soc.* **2002**, *124*, 12104–12105; b) T. G. Back, Z. Moussa, *J. Am. Chem. Soc.* **2003**, *125*, 13455–13460; c) T. G. Back, Z. Moussa, M. Parvez, *Angew. Chem. Int. Ed.* **2004**, *43*, 1268–1270; d) D. J. Press, E. A. Merceir, D. Kuzma, T. G. Back, *J. Org. Chem.* **2008**, *73*, 4252–4255.
[11] S.-C. Yu, A. Borchert, H. Kuhn, I. Ivanov, *Chem. Eur. J.* **2008**, *14*, 7066–7071.
[12] a) R. Déziel, E. Malenfant, G. Bélanger, *J. Org. Chem.* **1996**, *61*, 1875–1876; b) L. Uehlin, G. Fragale, T. Wirth, *Chem. Eur. J.* **2002**, *8*, 1125–1133; c) T. G. Back, Z. Moussa, M. Parvez, *J. Org. Chem.* **2002**, *67*, 499–509; d) M. Iwaoka, H. Komatsu, T. Katsuda, S. Tomoda, *J. Am. Chem. Soc.* **2002**, *124*, 1902–1909; e) M. Tiecco, L. Testaferri, C. Santi, C. Tomassini, F. Marini, L. Bagnoli, A. Temperini, *Chem. Eur. J.* **2002**, *8*, 1118–1124; f) M. Tiecco, L. Testaferri, C. Santi, C. Tomassini, F. Marini, L. Bagnoli, A. Temperini, *Angew. Chem.* **2003**, *115*, 3239–3241; *Angew. Chem. Int. Ed.* **2003**, *42*, 3131–3133; g) H. Poleschner, K. Seppelt, *Chem. Eur. J.* **2004**, *10*, 6565–6574; h) S. S. Khokhar, T. Wirth, *Angew. Chem.* **2004**, *116*, 641–643; *Angew. Chem. Int. Ed.* **2004**, *43*, 631–633; i) S. S. Khokhar, T. Wirth, *Eur. J. Org. Chem.* **2004**, 4567–4581; j) T. G. Back, Z. Moussa, M. Parvez, *Phosphorus, Sulfur Silicon Relat. Elem.* **2004**, *179*, 2569–2579; k) K. Okamoto, Y. Nishibayashi, S. Uemura, A. Toshimitsu, *Tetrahedron Lett.* **2004**, *45*, 6137–6139; l) M. Tiecco, L. Testaferri, C. Santi, C. Tomassini, R. Bonini, F. Marini, L. Bagnoli, A. Temperini, *Org. Lett.* **2004**, *6*, 4751–4753; m) M. Iwaoka, T. Katsuda, H. Komatsu, S. Tomoda, *J. Org. Chem.* **2005**, *70*, 321–327; n) K. Okamoto, Y. Nishibayashi, S. Uemura, A. Toshimitsu, *Angew. Chem. Int. Ed.* **2005**, *44*, 3588–3591; o) M. Tiecco, L. Testaferri, F. Marini, S. Sternativo, C. Santi, L. Bagnoli, A. Temperini, *Eur. J. Org. Chem.* **2005**, 543–551; p) A. D. Jones, A. L. Redforn, D. W. Knight, I. R. Morgan, A. C. Williams, *Tetrahedron* **2006**, *62*, 9247–9257.
[13] H. Poleschner, K. Seppelt, *Angew. Chem. Int. Ed.* **2008**, *47*, 6461–6464.
[14] a) H. Fujihara, H. Mima, N. Furukawa, *J. Am. Chem. Soc.* **1995**, *117*, 10153–10154; b) S. E. Denmark, W. R. Collins, M. D. Cullen, *J. Am. Chem. Soc.* **2009**, *131*, 3490–3492.
[15] D. Kuzma, M. Parvez, T. G. Back, *Org. Biomol. Chem.* **2007**, *5*, 3213–3217.
[16] a) G. Mugesh, A. Panda, H. B. Singh, R. J. Butcher, *Chem. Eur. J.* **1999**, *5*, 1411–1421; b) G. Mugesh, H. B. Singh, *Acc. Chem. Res.* **2002**, *35*, 226–236; c) S. S. Zade, H. B. Singh, R. J. Butcher, *Angew. Chem. Int. Ed.* **2004**, *43*, 4513–4515; d) S. S. Zade, S. Panda, S. K. Tripathi, H. B. Singh, G. Wolmershäuser, *Eur. J. Org. Chem.* **2004**, 3857–3864; e) S. S. Zade, S. Panda, H. B. Singh, R. B. Sunoj, R. J. Butcher, *J. Org. Chem.* **2005**, *70*, 3693–3704; f) S. Panda, S. S. Zade, H. B. Singh, G. Wolmershäuser, *J. Organomet. Chem.* **2005**, *690*, 3142–3148; g) S. K. Tripathi, U. Patel, D. Roy, R. B. Sunoj, H. B. Singh, G. Wolmershäuser, R. J. Butcher, *J. Org. Chem.* **2005**, *70*, 9237–9247; h) S. Sharma, K. Selvakumar, V. P. Singh, S. S. Zade, H. B. Singh, R. J. Butcher, *Phosphorus Sulfur Silicon Relat. Elem.* **2008**, *183*, 827–839.
[17] a) D. Sureshkumar, V. Ganesh, S. Chandrasekaran, *J. Org. Chem.* **2007**, *72*, 5313–5319; b) M. S. Korobov, V. I. Minkin, L. E. Nivorozhkin, *Zurnal Organicheskoi Khim.* **1975**, *11*, 826–831.
[18] a) M. J. Parnham, J. Biedermann, Ch. Bittner, N. Dereu, S. Leyck, H. Wetzig, *Agents Actions* **1989**, *27*, 306–308; b) B. Dakova, L. Lamberts, M. Evers, N. Dereu, *Electrochim. Acta* **1991**, *36*, 631–637.
[19] a) H. Fischer, N. Dereu, *Bull. Soc. Chim. Belg.* **1987**, *96*, 757–768; b) T. G. Back, B. P. Dyck, *J. Am. Chem. Soc.* **1997**, *119*, 2079–2083; c) B. K. Sharma, G. Mugesh, *Chem. Eur. J.* **2008**, *14*, 10603–10614.
[20] a) A. Bondi, *J. Phys. Chem.* **1964**, *68*, 441–451; b) L. Pauling, in: *The Nature of the Chemical Bond*, 3rd ed., Cornell University Press, Ithaca, New York, **1960**.
[21] L. Dupont, O. Dideberg, M. Sbit, N. Dereu, *Acta Crystallogr., Sect. C Cryst. Struct. Commun.* **1988**, *44*, 2159–2161.
[22] M. Iwaoka, S. Tomoda, *J. Am. Chem. Soc.* **1996**, *118*, 8077–8084.
[23] T. K. Zywietz, H. Jiao, P. von R. Schleyer, A. de Meijere, *J. Org. Chem.* **1998**, *63*, 3417–3422.
[24] See Table S19 in the Supporting Information for the NICS calculations.
[25] H. J. Reich, W. W. Willis, S. Wollowitz, *Tetrahedron Lett.* **1982**, *23*, 3319–3322.
[26] a) J. L. Kice, T. W. S. Lee, *J. Am. Chem. Soc.* **1978**, *100*, 5094–5102; b) J. L. Kice, D. W. Purkiss, *J. Org. Chem.* **1987**, *52*, 3448–3451.
[27] D. D. Perrin, W. L. F. Armarego, *Purification of Labratory Chemicals*, Pergamon Press, 4th ed., **1996**.
[28] L. K. A. Rahman, R. M. Scrowston, *J. Chem. Soc. Perkin Trans. 1* **1984**, 385–390.
[29] M. J. Frisch, G. W. Trucks, H. B. Schlegel, G. E. Scuseria, M. A. Robb, J. R. Cheeseman, J. A. Montgomery Jr, T. Vreven, K. N. Kudin, J. C. Burant, J. M. Millam, S. S. Iyengar, J. Tomasi, V. Barone, B. Mennucci, M. Cossi, G. Scalmani, N. Rega, G. A. Petersson, H. Nakatsuji, M. Hada, M. Ehara, K. Toyota, R. Fukuda, J. Hasegawa, M. Ishida, T. Nakajima, Y. Honda, O. Kitao, H. Nikai, M. Klene, X. Li, J. E. Knox, H. P. Hratchian, J. B. Cross, V. Bakken, C. Adamo, J. Jaramillo, R. Gomperts, R. E. Stratmann, O. Yazyev, A. J. Austin, R. Commi, C. Pomelli, J. W. Ochterski, P. Y. Ayala, K. Morokuma, G. A. Voth, P. Salvador, J. J. Dannenberg, V. G. Zakrazewski, S. Dapprich, A. D. Daniels, M. C. Strain, O. Farkas, D. K. Malick, A. D. Rabuck, K. Raghabachari, J. B. Foresman, J. V. Ortiz, Q. Cui, A. G. Baboul, S. Clifford, J. Cioslowski, B. B. Stefanov, G. Liu, A. Liashenko, P. Piskorz, I. Komaromi, R. L. Martin, D. J. Fox, T. Keith, M. A. Al-Laham, C. Y. Peng, A. Nanayakkara, M. Challacombe, P. M. W. Gill, B. Johnson, W. Chen, M. W. Wong, C. Gonzalez, J. A. Pople, *Gaussian 03*, Revision C.02, Gaussian, Inc., Wallingford, CT, **2004**.
[30] a) C. Lee, W. Yang, R. G. Parr, *Phys. Rev. B* **1988**, *37*, 785–789; b) A. D. Becke, *J. Chem. Phys.* **1993**, *98*, 5648–5652.
[31] C. A. Bayse, *Inorg. Chem.* **2004**, *43*, 1208–1210.
[32] a) A. E. Reed, L. A. Curtiss, F. Weinhold, *Chem. Rev.* **1988**, *88*, 899; b) F. Weinhold, *Natural Bond Orbital (NBO)*, version 5.0.
[33] a) P. von R. Schleyer, C. Maerker, A. Dransfeld, H. Jiao, N. J. R. van E. Hommes, *J. Am. Chem. Soc.* **1996**, *118*, 6317–6318; b) P. von R. Schleyer, M. Manoharan, Z.-X. Wang, B. Kiran, H. Jiao, R. Puchta, N. J. R. van E. Hommes, *Org. Lett.* **2001**, *3*, 2465–2468; c) Z. Chen, C. S. Wannere, C. Corminboeuf, R. Puchta, P. von R. Schleyer, *Chem. Rev.* **2005**, *105*, 3842–3888; d) E. Kleinpeter, S. Klod, A. Koch, *THEOCHEM* **2007**, *811*, 45–60.
[34] G. M. Sheldrick, *SHELXL-97*, *Program for Crystal Structure Determination*, University of Göttingen, Germany, **1997**.

Received: July 16, 2009
Published Online: December 16, 2009

